Integrative and Comparative Biology

Integrative and Comparative Biology, volume 59, number 3, pp. 716–730
doi:10.1093/icb/icz115

Society for Integrative and Comparative Biology

SYMPOSIUM

Building a Body Shape Morphospace of Teleostean Fishes

S. A. Price,[1,*] S. T. Friedman,[†] K. A. Corn,[†] C. M. Martinez,[†] O. Larouche[*] and P. C. Wainwright[†]

[*]Department of Biological Sciences, Clemson University, Clemson, SC 29634, USA; [†]Department of Evolution and Ecology, University of California Davis, Davis, CA 95616, USA

From the symposium "Comparative Evolutionary Morphology and Biomechanics in the Era of Big Data" presented at the annual meeting of the Society for Integrative and Comparative Biology, January 3–7, 2019 at Tampa, Florida.

[1]E-mail: sprice6@clemson.edu

Synopsis We present a dataset that quantifies body shape in three dimensions across the teleost phylogeny. Built by a team of researchers measuring easy-to-identify, functionally relevant traits on specimens at the Smithsonian National Museum of Natural History it contains data on 16,609 specimens from 6144 species across 394 families. Using phylogenetic comparative methods to analyze the dataset we describe the teleostean body shape morphospace and identify families with extraordinary rates of morphological evolution. Using log shape ratios, our preferred method of body-size correction, revealed that fish width is the primary axis of morphological evolution across teleosts, describing a continuum from narrow-bodied laterally compressed flatfishes to wide-bodied dorsoventrally flattened anglerfishes. Elongation is the secondary axis of morphological variation and occurs within the more narrow-bodied forms. This result highlights the importance of collecting shape on three dimensions when working across teleosts. Our analyses also uncovered the fastest rates of shape evolution within a clade formed by notothenioids and scorpaeniforms, which primarily thrive in cold waters and/or have benthic habits, along with freshwater elephantfishes, which as their name suggests, have a novel head and body shape. This unprecedented dataset of teleostean body shapes will enable the investigation of the factors that regulate shape diversification. Biomechanical principles, which relate body shape to performance and ecology, are one promising avenue for future research.

Introduction

Teleosts are an eminently successful vertebrate radiation. Originating around 310–350 million years ago (mya), according to molecular estimates (Miya et al. 2010; Near et al. 2012) following a whole genome duplication (Hoegg et al. 2004; Vandepoele et al. 2004), there are now approximately 31,000 living teleost species (Fricke et al. 2019). Teleost fishes occupy almost every aquatic habitat on earth, from coral reefs and open ocean, rivers, and lakes, through to abyssal ocean trenches and isolated hot springs (Helfman et al. 2008). Perhaps reflecting their ecological diversity teleosts also exhibit a spectacular variety of body shapes, which range from deep-bodied (e.g., moonfish, spadefish), elongate (e.g., eels, needlefish), laterally compressed (e.g., ribbonfish) to globular (e.g., pufferfish), plus uniquely shaped groups like seahorses, flatfishes, and ocean sunfishes.

How can we begin to understand how and why the remarkable diversity of fish body forms evolved? The selective pressures on body shape are undoubtedly highly complex and interconnected but taking into consideration biomechanical principles can help, as they link shape to performance, which in turn are tied to evolutionary fitness and thus can be acted upon by natural selection (Arnold 1983). The performance that maximizes fitness depends on the environmental and ecological context. For example, swimming performance depends on the net balance between thrust and resistance, which is determined by hydrodynamic properties of body shape (as reviewed by Webb 1984, 1997; Domenici 2002; Langerhans and Reznick 2010). Cruising (sustained swimming for an hour or more) requires the maximization of thrust and the minimization of drag, which is achieved with a streamlined fusiform shape with a narrow caudal region that reduces side-forces, as exemplified by tunas (Scombridae). In contrast, maneuverability is enhanced by deepening, shortening, and laterally compressing the body, as this shape

Advance Access publication June 26, 2019

offers the least resistance to rotation in the median vertical plane of the body (Webb 1984), as demonstrated by butterflyfishes (Chaetodontidae). Body shapes that increase maneuverability or cruising performance preclude similar improvements in the other performances (Weihs 1993; Webb 1997) due to trade-offs (although see Blake et al. 1995; Blake 2004). Therefore, fishes living in open water, where food/mating partners are dispersed and there are few obstacles, are expected to evolve fusiform shapes suited for sustained cruising. While fishes living in complex habitats are expected to evolve shapes that improve maneuverability (Webb 1984, 1997; Langerhans and Reznick 2010). As we expect interactions between different aspects of ecology (e.g., diet and habitat) and the environment (e.g., salinity and water temperature), as well as trade-offs between various performances (e.g., locomotor and feeding performance), body shape ultimately represents a compromise between competing forces constrained by historical factors.

Surprisingly, given the obvious diversity of fish body shapes and the strong predictions relating form to ecology, there have been no attempts to comprehensively explore general patterns and repeating themes in the relationship between body shape, functional morphology, and ecology across teleost fishes. Despite textbook examples and the general acceptance of rampant body shape convergence across fishes (e.g., Moyle and Chech 2004; Helfman et al. 2008) it is not clear what the dominant axes of body form diversity are, and whether they can be explained by ecology. Elongation, the anteroposterior lengthening of a fish relative to other body dimensions, has been identified as the primary axis of diversification across a broad sample of reef fishes (Claverie and Wainwright 2014). However, this previous study lacks information on width and it is focused on reef fishes, which may be a biased sample of fish body plans, as complex structured environments are expected to select for deep-bodied laterally compressed shapes. At small scales, many studies demonstrate an effect of ecology on fish body shape within and between species. For example, intraspecific experiments have identified consistent adaptive plastic responses to being fed zooplankton, whereby the body develops a more streamlined form (e.g., Andersson 2003; Andersson and Johansson 2006). Studies within and between natural populations have found similar changes in shape in response to ecological differences (Lavin and Mcphail 1985; Robinson et al. 1993; Langerhans and Chapman 2007; Langerhans et al. 2007). Genetic studies within benthic–limnetic three-spined stickleback reveal that the adaptive shape shift appears to be driven by a few quantitative trait loci of large effect size (Albert et al. 2008). Such genetic divergence or plastic responses to common environmental gradients can drive microevolutionary change, speciation, and thus convergence (e.g., West-Eberhard 2005; Ghalambor et al. 2007).

The few macroevolutionary studies conducted on teleost clades, most notably African rift lake cichlid radiations, support the link between ecology and body shape by identifying morphological convergence associated with trophic and habitat similarities (e.g., Clabaut et al. 2007; Muschick 2012; Frédérich et al. 2013; Davis et al. 2014). However, to quantitatively investigate how complex interactions between ecological and environmental factors shape fish body form at the macroevolutionary scale requires vast amounts of data spanning large taxonomic scales. To illustrate why we need such large datasets, suppose we are interested in the interaction between diet and habitat complexity and how it influences shape. If we categorize diet and habitat complexity into three states of interest each, we need multiple evolutionary independent origins of each of the nine combinations of diet and habitat state. These are our natural evolutionary experiments which ensure any pattern between ecology is not driven by phylogenetic pseudo-replication (Felsenstein 1985). As ecological and morphological traits are phylogenetically conserved transitions between states are relatively rare, and so to encompass enough independent associations between each state combination the macroevolutionary dataset needs to span large taxonomic scales. Therefore, generating vast trait databases, not only allows us to investigate the general patterns of macroevolution within the clade but also to incorporate more realistic complexity into our evolutionary models (Chira et al. 2018).

The ready availability of large genetic datasets is driving increased interest in generating matching phenotypic and ecological databases within the disciplines of genomics (Houle et al. 2010) and macroevolution (Chang and Alfaro 2016). Recently, novel macroevolutionary insights have been gained by harnessing the power of crowdsourcing to place geometric morphometric landmarks 3D scans of bird beaks (Cooney et al. 2017; Chira et al. 2018) and similar methods have been established for placing landmarks on lateral photographs of fish (Chang and Alfaro 2016). We quantify the teleost body shape space using a dataset of functionally relevant linear shape variables, which we generated with a team of trained researchers taking measurements with hand-held calipers. We took this approach as we wanted

measurements in all three functionally relevant dimensions: lengths, depths, and widths. However, 3D scanning techniques would have been difficult to implement due to specimen distortion (e.g., bending) from preservation. Our data collection required a large number of people to measure museum specimens, so we utilized undergraduate researchers, whom we recruited into an 18-month long research program that enabled them to experience the entire process of science through practice. We briefly outline the design of this undergraduate research experience in the "Materials and methods" section. In addition to presenting the teleostean morphospace we also estimate the tempo of morphological diversification across teleost fishes, to identify families with the highest rates of evolution. Throughout, we discuss some of the issues we encountered when building and analyzing the dataset, highlighting some of the promises and pitfalls of big-data approaches.

Materials and methods

Data

Collection

Data were collected at the Smithsonian National Museum of Natural History fish collections over 7 months during the summers of 2016, 2017, and 2018 by a large team of researchers, including the authors of this paper and many others (listed with an asterisk in the "Acknowledgments" section). All researchers had at least 3 months of training using the data collection protocols. Where possible we measured three specimens per species to measure and we picked the most intact specimens of adult size that were preferably collected at different times and places to encompass some spatial and temporal variation. We measured eight easy-to-identify, ecologically and functionally relevant shape variables (Supplementary Fig. S1). *Standard length* (mm): the straight-line distance from the most anterior tip of the upper jaw to the mid-lateral posterior edge of the hypural plate (in fishes with a hypural plate), or to the posterior end of the vertebral column in fishes lacking them (i.e., excluding the caudal fin). This was identified by manipulating the specimen and looking for a wrinkle on the caudal peduncle when the caudal region is flexed. *Maximum body depth* (mm): the greatest depth measured by a straight-line distance from dorsal to ventral surface of the body, with body defined as the region posterior to the operculum and anterior to the caudal peduncle. *Maximum fish width* (mm): the width of the fish measured at its maximum anywhere on the specimen. *Head depth* (mm): the vertical distance from dorsal to ventral surface of the head passing through the pupil of the eye. *Lower jaw length* (mm): length of the mandible from the anterior end of the lower jaw to the articular–quadrate joint. *Mouth width* (mm): the width of the fish measured at the distance between the left and right articular–quadrate joints. The articular–quadrate joint was identified by feeling for the joint, along with moving the lower jaw and identifying the point where the movement stopped. Occasionally, when the jaw wouldn't move, we estimated the position of the joint by inferring it from the end of the opercular slit. The method used to identify the joint was noted in the datasheet. *Minimum caudal peduncle depth* (mm): the depth measured by a straight-line distance from dorsal to ventral surface of the caudal peduncle at its shallowest point. *Minimum caudal peduncle width* (mm): the width of the fish measured at its narrowest point on of the caudal peduncle. Measurements were made on every specimen, unless part of the specimen was missing or damaged in a manner precluding the measurement of a particular trait. We also photographed and weighed each specimen as well as measuring the first major spine and longest spine in every fin; however, we will not discuss these data further in this paper. All linear measurements were taken with handheld dial or digital calipers with a minimum accuracy of 0.1 mm unless the fish was over 30 cm in length, in which case, we used a measuring tape with a minimum accuracy of 1 mm. We were unable to weigh the largest specimens as we had no scales to accommodate them. Additionally, our scales had a minimum accuracy of 1 g so we were also unable to weigh the very smallest specimens. In total, 16,609 specimens were measured.

Data cleaning

The data were carefully checked for problems, such as typos or misreading the calipers using a three-step process coded in R. Briefly, the first step was at the species-level, any species with more than our maximum of three specimens was identified and the specimen number checked to ensure that they were listed as the correct species. We then calculated the standard deviation among specimens for each species after dividing each trait by the standard length of the specimen, 0.1 was set as the minimum acceptable within-species standard deviation. We also checked for issues where the max body width was less than the mouth width and, likewise, the head depth deeper than the maximum body depth. The second step was at the genus-level, all traits were divided by the standard length of the specimen and outlier

specimens within a genus were identified using interquartile ranges (IQR), specifically if $x <$ quantile(x, 0.05)-1.5 * IQR(x) or $x >$ quantile(x, 0.95) + 1.5 * IQR(x). For a given trait, if all three specimens of a species were listed as outliers, these were considered normal morphological variation and thus not added to a document for manual inspection. If not, they were added to the document and underwent further examination based on the photographs. The third step was at the family-level, following the same protocol described for the generic level, but this time we found outlying specimens relative to their respective families. Specimens from monotypic families were manually checked for erroneous measurements. When possible, erroneous measurements were replaced with new measurements taken on the photograph of the specimen using ImageJ (Rueden et al. 2017). All remaining outliers that we could not verify were removed from the dataset. Once we had removed all potential issues, averages of each trait value were taken across specimens within a given species. A total of 6144 species remained following data cleaning.

Phylogeny

In order to be able to analyze our data in a phylogenetic framework we targeted species that were represented by genetic sequence data and were included in a large phylogeny of fishes (Rabosky et al. 2013, 2018). The species names listed on measured specimens were matched to the phylogeny using fishbase (Froese and Pauly 2019) and catalog of fishes (Fricke et al. 2019). For the analyses, the morphological dataset was pruned to match the species in Rabosky et al. (2018) and species that had missing data were also removed, leaving 5881 species.

All of the phylogenetic comparative analyses we implemented assume a Brownian motion model of evolution. Under this model, trait variance is proportional to time. This means that very short branch lengths, specifically at the tips of the tree can bias comparative analyses. In particular, the rates of morphological change may be overestimated over short-time intervals, especially if there is measurement error (Martins 1994). To look for issues generated by short branches we calculated standardized phylogenetic independent contrasts (Felsenstein 1985), which can be viewed as phylogenetically correct estimates of the rate of morphological evolution (Garland 1992). The top 0.5% of contrasts were identified for each trait using both methods of size correction (see next section) and the node ages of these contrasts were identified (Supplementary Table S1). The majority (70%) of these high rate contrasts came from sister-species that last shared a common ancestor <0.1 mya, this is particularly true for the largest contrasts, as 97% of the top 10 contrasts have node ages <0.1 mya. The Rabosky et al. (2018) phylogeny contains 31 species pairs that share a most recent common ancestor <0.1 mya (Supplementary Table S2). While these species may represent extraordinarily rapid evolutionary change, the short branches will amplify the effect of any potential measurement error and have the potential overwhelm the overall signal within the data. To prevent these very recent divergences from having undue influence on the results, one species from each pair was removed, leaving a total of 5850 species representing 390 families, for the final analyses.

Analyses

Size correction

Our dataset contains specimens ranging from 10 to 1760 mm in length, thus differences in size will dominate most of our body shape measurements. For example, a tuna is going to have a longer lower jaw and deeper body than a goby because it is a much larger fish. Therefore, the effects of size and shape need to be separated but exactly how this is done has been the subject of much debate (see reviews by Jungers et al. 1995; Klingenberg 1996, 2016). The impact of size on shape can be divided into isometry and allometry. For example, a goby scaled-up to the size of a tuna may have the same jaw length and body depth measurements as the tuna (isometry). Alternatively, shape may change predictably with size such that the goby scaled-up to the size of a tuna will have predictably deeper or shallower depth measurements than the tuna based on its initial size (positive or negative allometry). We implement two commonly used but philosophically different methods of size correction (Klingenberg 1996, 2016), to investigate how the choice of size correction influences down-stream evolutionary analyses. The two methods of size correction differ in three important aspects: (1) whether variance due to allometry is retained following size correction, (2) whether the phylogenetic context is taken into account during size correction, and (3) whether the size of a fish is accurately represented by a single measurement or not.

Many macroevolutionary studies that implement phylogenetic comparative analyses size correct their data by taking the residuals from a phylogenetic regression of each variable against size (Garland et al. 1992; Revell 2009). Using these residuals removes the variance associated with evolutionary allometry,

regardless of whether there is direct proportionality between shape and size and therefore potentially removing both allometric and isometric components of size. In ichthyological studies either standard length, total length, or fork length are used as the measure of size, as lengths are less affected by body condition than mass. This holds true for museum specimens, in which length decreases far less than mass during preservation in ethanol or formaldehyde (Kristoffersen and Salvanes 1998). Moreover, specimens are frequently incomplete, with tissue samples or digestive and reproductive tracts removed, which again affects mass more than it does length. We calculated the residuals from the phylogenetic regression of log standard length (hereafter referred to SL residuals) using the method outlined by Revell (2009) and implemented in the R package phytools (Revell 2012). We also investigated the slopes of phylogenetic regressions across all species using the caper package in R (Orme et al. 2018).

An alternative method for size-correction, more akin to those employed in geometric morphometric analyses, is to scale each variable by the geometric mean of the variables and to take the log of those values, generating log shape ratios (Mosimann 1970; Klingenberg 2016). Size is a complex concept and this method removes the need to pick a single variable to represent size by using the geometric mean as a composite measure. Moreover, it should preserve the allometric aspects of shape that change as a function of size (Klingenberg 2016). Log-shape ratios were calculated in R following the method outlined in Claude (2013): each variable was divided by the size of the species as calculated by the geometric mean of the three main size dimensions of a fish: standard length, maximum body depth and maximum fish width, and log-transforming the resulting value. We chose not to calculate size as the geometric mean of all measured traits, as our dataset contains three traits that are inclusive estimates of the three major dimensions of size and all of the other traits are smaller valued width, depth, and length measurements nested within them.

Principal components analysis

In order to identify the primary axes of shape variation we visualized fish body morphospace by performing a principal component analysis on the log-standard length residuals and the log–shape ratios. As one degree of freedom is lost due to scaling when using shape ratios (Claude 2013) only the first seven instead of the eight principal component scores describe the shape variation in the dataset. All analyses were conducted on the correlation matrix. The correlation matrix is recommended when the variance and range are different within the data or if it makes biological sense that the variables with high or low variance contribute equally to the primary axes of variation. The original variables vary in scale, but we are generating the morphospaces using size-corrected variables, which are either the residuals from the regression against log standard length or the log of the variable divided by the geometric mean. We would therefore expect them to exhibit more similar ranges and much lower variance than the original variables. This is true for the residuals from the phylogenetic regression, but the log shape ratios generate a couple of variables with quite different ranges, and these dominate PC1 if a covariation matrix is used. Therefore, we chose to use the correlation matrix to generate all our morphospaces.

We used a phylogenetic PCA implemented in the R package phytools (see Revell 2009), this identifies the major axes of variation once phylogenetic covariation has been removed thus preventing unusually shaped clades from potentially dominating the axes. However, it is important to recognize that the morphospace plots on the scores from the phylogenetic PCA still contain a significant phylogenetic component (Revell 2009; Polly et al. 2013). To examine the effect of common ancestry on the major axes of variation a non-phylogenetic PCA is provided in the Supplementary Materials (Supplementary Fig. S2 and Supplementary Tables S3 and S4). Additionally, to examine the impact on the morphospace we also repeated the phylogenetic PCAs using log shape ratios calculated using the geometric mean of all traits and the results are available in the Supplementary Materials (Supplementary Table S5).

Rates of body shape change

To identify families that exhibit particularly high rates of body shape change we estimated the Brownian rate of evolution of each size-corrected shape trait as well as size (either standard length or the geometric mean) within each family with at least 10 species in our dataset, using the fitContinuous function in the R package Geiger (Pennell et al. 2014). The rate differences among families and variables were then visualized on a family-level phylogeny using the phylo.heatmap function in the phytools package (Revell 2012). Each variable was standardized to have the same mean and variance.

Undergraduate research experience

Our intention when developing this experience was to combine the positive aspects of generating a peer-group cohort (e.g., Zhao and Kuh 2004;

Auchincloss et al. 2014) with undergraduate research, as well as to promote the development of critical thinking skills, self-confidence, analytical capabilities, scientific writing, and presentation-giving, all of which can create pathways to science careers (e.g., Seymour et al. 2004; Lopatto 2007, 2009; Gormally et al. 2009). Three cohorts of between 10 and 19 students learned and worked together for 18 months (either three semesters at Clemson University or four quarters at UC Davis) during which time they earned research credit. Each group worked together to design and execute an ambitious common research project based on the data they helped to collect, with the ultimate goal of publishing the results.

During the first section, students were introduced to the overall project, its goals and the data that are being collected. They received hands-on training, working with fish specimens to learn to our specific measurements and identify basic morphology. They learned how to use bibliographic search engines to find relevant scientific papers and how to read the papers. Students then used these skills to identify and develop interesting questions that were testable with the body shape data they helped to collect. With guidance from their mentors and after several rounds of proposals, peer-review and in-class debates a suitable scientific hypothesis was identified and specific predictions developed. In the second section the students focused on learning how to analyze the data. Using the R statistical framework, they were taught basic programming, data visualization, and statistical methods including the phylogenetic comparative methods they would need to answer their specific questions. During the final section the students finished analyzing and interpreting the data and worked on presenting their findings at local conferences in the form of a scientific poster or talk and started to plan the paper for publication.

As undergraduate research experience has been shown to be a critical factor when choosing to pursue a career in science, especially for students from traditionally underrepresented groups (e.g., Lopatto 2007; Villarejo et al. 2008), we aimed to make our recruitment and program inclusive. We targeted students who had no previous research experience by advertising widely across campus and by taking advantage of campus programs targeted toward first generation and minority students. We met with every potential recruit individually to talk to them about the project and to determine their enthusiasm and suitability for the program, rather than focusing purely on an application letter and grades, a practice that may also improve the recruitment of minority candidates (Gándara 1999). We also provided paid research positions during the summer ensuring that the opportunity to work at the Smithsonian museum was open to all students, not just those that could afford to take an unpaid internship for a month.

Results

Size correction

Correcting for size using the residuals from the phylogenetic regression with log standard length means that length itself cannot be included as a shape variable. This is unfortunate as elongation, the lengthening of the body relative to other dimensions, has been shown to be the primary axis of variation across reef fishes using geometric morphometric approaches (Claverie and Wainwright 2014). However, as the residuals represent every trait relative to standard length, elongation can be identified by narrower widths and shallower depths than expected for their length, i.e., negative residuals. Indeed, there is a strong positive relationship between the SL residuals for width and depth. Across the eight variables, phylogenetic slopes from regressions on log standard length were: maximum body depth ($\beta = 1.15$), maximum fish width ($\beta = 1.09$), head depth ($\beta = 1.04$), lower jaw length ($\beta = 0.95$), mouth width ($\beta = 1.03$), minimum caudal peduncle depth ($\beta = 1.02$), and minimum caudal peduncle width ($\beta = 1.15$). These estimates indicate that across teleost fishes shape variables change in proportion to standard length and that the estimated evolutionary allometry is close to isometry ($\beta = 1$) for most traits, although there is a lot of variation around the phylogenetic regression line.

Size-correction using log-shape ratios allows us to include standard length, where fishes that are elongate will have the largest size-corrected standard lengths. If fishes that are long for their overall size are also shallower and/or narrower this would provide further evidence of elongation. There is a significant negative relationship between size-corrected standard length and body depth in both the non-phylogenetic and phylogenetic analyses ($\beta = -0.68$ and $P < 2e^{-16}$, PGLS $\beta = -0.54$ and $P < 2e^{-16}$) with the adjusted R^2 values indicating standard length explains between 30% and 47% of the variation in size-corrected depth. For body width there is also a significant negative relationship in both the non-phylogenetic and phylogenetic analyses ($\beta = -0.32$ and $P < 2e^{-16}$, PGLS $\beta = -0.46$ and $P = P < 2e^{-16}$) but the adjusted R^2 values indicate standard length only explains 15–25% variation in size-corrected width. As expected, there is a positive

relationship between the log-shape ratios and the SL residuals for each variable (Klingenberg 1996) (see Supplementary Fig. S3).

Principal components analysis

PC1 represents the phylogenetically weighted major axis of body shape divergence across teleosts. For the SL residuals all traits except lower jaw length load relatively heavily onto this major axis (see Table 1 and Fig. 1). Usually this would indicate that PC1 is driven by size but as we have removed size using standard length it is actually an axis that is strongly associated with elongation, as it represents the reduction of body dimensions relative to standard length. PC1 therefore characterizes a continuum of fishes from deep and wide-bodied Lophiiformes (anglerfishes) to long, narrow, and shallow Anguilliformes (eels). The secondary axis of variation contrasts fishes with small mouths and deep and wide caudal peduncles, like many of the Monacanthidae and Cobitidae, with fishes like the Macrouridae, Zoarcidae, and Trichiuridae that have larger mouths and thin, shallow peduncles. PC1 explains 45.3% of the total body shape variation and PC2 explains a further 16.6%. PC3 and 4 together explain an additional 22% of the shape variation. PC3 describes a continuum, at one extreme fishes with long lower jaws and relatively wide caudal peduncles like the Belonidae and at the other extreme are Gymnotiformes (knifefishes) and Macrouridae, with relatively short lower jaws and narrow caudal peduncles. While PC4 contrasts lower jaw length and mouth width, where the narrow-mouthed but relatively long-jawed Pleuronectiformes (flatfishes) and Carangidae occupy one extreme, with Loricariidae at the other having wide but relatively short mouths.

The major axes of body shape variation identified using the log-shape ratios differ somewhat from those identified using the SL residuals (see Table 2 and Fig. 1). The first principal component axis is width, wide dorsoventrally flattened Lophiiformes are at one extreme and narrow laterally compressed Pleuronectiformes at the other. PC2 contrasts standard length with body depth with long shallow fishes like the Anguilliformes at one extreme and short deep fishes like Ephippidae and Caproidae at the other. PC2 therefore represents an axis of elongation. The percentage of the total body shape variation explained by each PC axis is surprisingly even, PC1 only explains 22.6% of the total body shape variation, PC2 explains a further 21.8%. PC3 and 4 together explain an additional 31% of the shape variation. PC3 describes a continuum, at one extreme are fishes with deep and wide caudal peduncles like Notosudidae and Belonidae, and at the other extreme fishes with shallow and narrow caudal peduncles, like Macrouridae, Trichiuridae, and Gymnotiformes. While PC4 describes a continuum of morphologies from fishes with long lower jaws and relatively deep heads, such as Trichiuridae, Nemichthyidae, and Serrivomeridae, through to fishes like some Siluriformes (catfishes) and Ostraciidae that have short lower jaws and shallow heads relative to their width.

The decision to prune out the 31 species containing nodes that were <0.1 million years resulted in several changes in the major axes identified by the phylogenetic PCA (Supplementary Tables S6 and S7).

Rates of body shape change

Rates of body shape evolution vary substantially across the phylogeny (Fig. 2 and Supplementary Tables S8 and S9). Two families show high rates of

Table 1 Loadings and variance for the phylogenetic principal components analysis on log standard length residuals

	PC1	PC2	PC3	PC4	PC5	PC6	PC7
ln Max body depth	−0.800	0.136	−0.355	−0.242	0.136	−0.049	0.369
ln Max fish width	−0.802	−0.178	−0.152	0.276	−0.002	−0.449	−0.154
ln Head depth	−0.818	−0.025	−0.275	−0.197	0.206	0.290	−0.298
ln Lower jaw length	−0.406	−0.572	0.538	−0.459	0.023	−0.079	0.014
ln Mouth width	−0.640	−0.478	0.080	0.474	−0.199	0.272	0.134
ln Min caudal peduncle depth	−0.628	0.526	0.146	−0.176	−0.523	0.012	−0.053
ln Min caudal peduncle width	−0.500	0.524	0.540	0.254	0.342	0.024	0.028
Standard deviation	1.781	1.076	0.913	0.839	0.701	0.608	0.520
Proportion of variance	0.453	0.166	0.119	0.101	0.070	0.053	0.039
Cumulative proportion	0.453	0.619	0.738	0.838	0.909	0.961	1.000

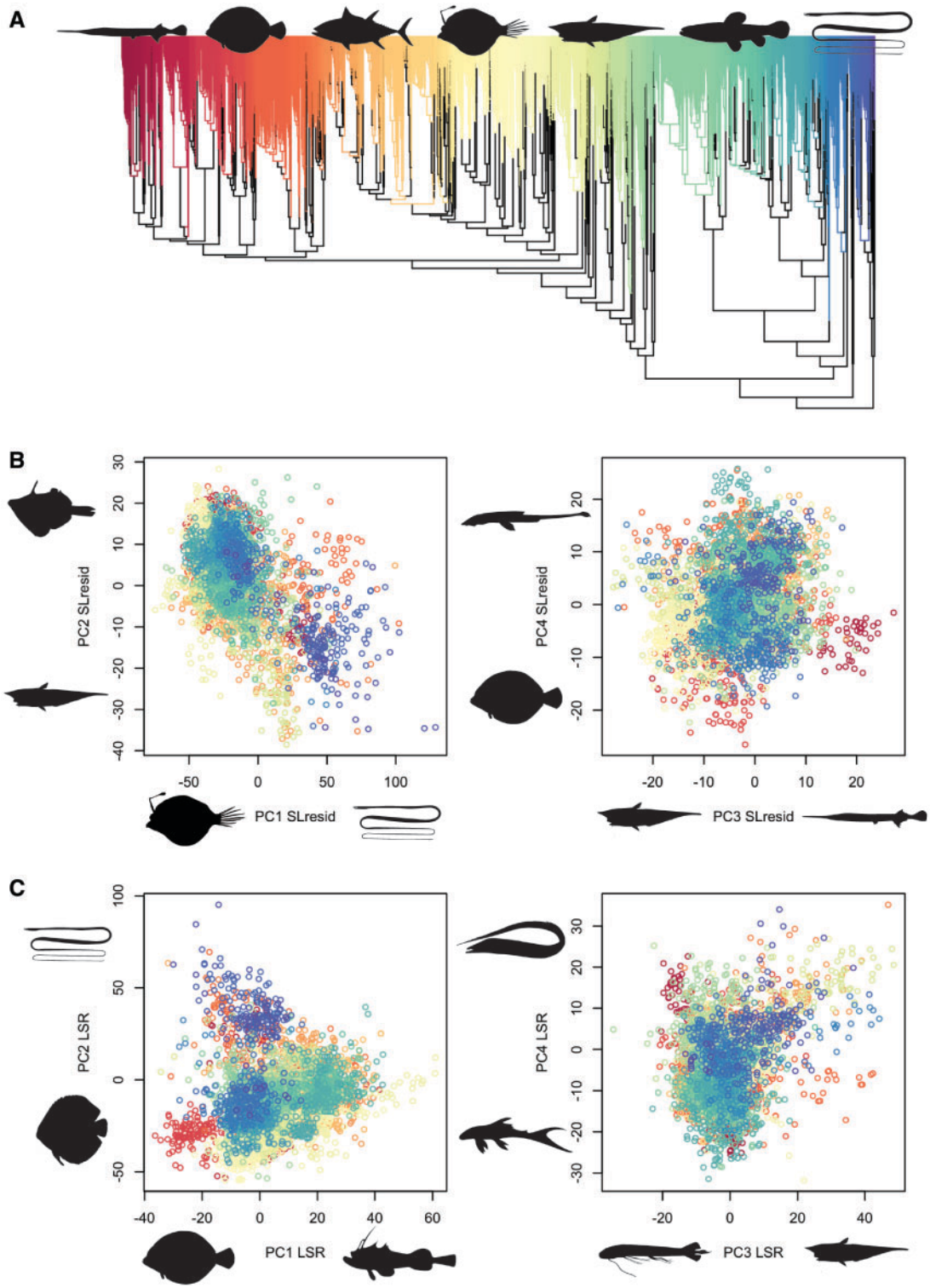

Fig. 1 Teleostean morphospace. **A**) (Rabosky et al. 2018) Phylogeny pruned to the 5850 species that overlap with the body shape dataset and excluding 31 species that share a common ancestor with their sister-species <0.1 mya. Each of the 390 families are represented by a different color and the same colors are used in the morphospaces (**B** and **C**) to give an idea of phylogenetic relationships, as a phylomorphospace is impractical with so many species. B) Plot of PC1 vs. PC2 and PC3 vs. PC4 using scores from the phylogenetic PCA on log standard length residuals (SLresids). C) Plot of PC1 vs. PC2 and PC3 vs. PC4 using the scores from the phylogenetic PCA on log-shape ratios (LSRs).

Table 2 Loadings and variance for the phylogenetic principal components analysis on log shape ratios

	PC1	PC2	PC3	PC4	PC5	PC6	PC7
Standard length	−0.477	0.790	−0.240	0.158	0.191	0.095	−0.145
Max body depth	−0.380	−0.812	0.311	0.109	−0.263	0.125	−0.052
Max fish width	0.903	0.004	−0.068	−0.281	0.070	−0.231	0.208
Head depth	−0.062	−0.508	−0.220	0.519	0.618	−0.059	0.187
Lower jaw length	0.141	0.154	−0.377	0.716	−0.487	−0.176	0.182
Mouth width	0.697	−0.162	−0.224	0.260	0.023	0.300	−0.529
Min caudal peduncle depth	−0.322	−0.338	−0.618	−0.286	−0.033	−0.468	−0.313
Min caudal peduncle width	−0.084	−0.191	−0.750	−0.334	−0.093	0.445	0.276
Standard deviation	1.344	1.320	1.159	1.076	0.860	0.787	0.768
Proportion of variance	0.226	0.218	0.168	0.145	0.092	0.077	0.074
Cumulative proportion	0.226	0.444	0.612	0.756	0.849	0.926	1.000

evolution (identified as >95th percentile) across several traits regardless of the method of size correction: Channichthyidae and Zoarcidae. When log-shape ratios are used Liparidae and Mormyridae also show high rates across three or more traits, while Stichaeidae and Triglidae are also identified as exhibiting high rates when SL residuals are used.

Some families reveal high rates of evolution in only one or two traits. Both methods of size correction identify high rates of lower jaw evolution in Chaetodontidae and high rates of mouth width evolution in Exocoetidae. SL residuals identify Cobitidae as having high rates of mouth evolution (lower jaw length and mouth width) while Catostomidae are likewise identified by log-shape ratios. Sebastidae, Salmonidae, Kyphosidae, and Channichthyidae are identified as having high rates of geometric mean evolution, while Belonidae, Triglidae, Scorpaenidae, and Tetraodontidae are identified as having high rates of standard length evolution.

These results are also dependent on the removal of the 31 sister-species nodes <0.1 mya. Without the removal of the nodes <0.1 mya the majority of families identified as exhibiting extraordinary rates are those that contain one or nodes <0.1 mya (Supplementary Fig. S4). This illustrates the importance of identifying and removing outliers.

Discussion

We have generated the largest macroevolutionary database of vertebrate morphology to date, with measurements on 16,609 specimens from a total of 6144 species in 394 families, representing just under a quarter of living teleostean diversity. Analyzing this dataset will help to bridge the gap between 1) microevolutionary studies that demonstrate how body shape changes are induced by different ecologies intraspecifically (e.g., Robinson et al. 1993; Andersson 2003; Andersson and Johansson 2006), 2) biomechanical principles that express how certain shapes optimize specific performance traits (e.g., Webb 1984; Domenici 2002; Weihs 2002), and 3) the remarkable body form diversity observed across the teleost tree of life. Its taxonomic span will also enable the incorporation of more realistic complexity within macroevolutionary models, allowing us to ask whether trait interactions and trade-offs constrain shape convergence.

Elongation is identified as a major axis of shape variation within teleost fishes regardless of the method of size correction: PC1 when residuals from the phylogenetic regression against standard length are used or PC2 when log shape ratios are used. In our analyses the precise role played by width and the amount of variation in shape variation explained by elongation depends strongly on which method of size correction is used. When SL residuals are analyzed PC1 explains 45.3% of the total variation and describes a continuum from deep and wide heads and bodies relative to their length through to highly elongate forms with relatively shallow and narrow heads and bodies. Within the morphospace most outlier species are ones with shallower or narrower body dimensions than expected for their length, i.e., are elongate. When log shape ratios are analyzed PC2 describes the elongation axis (see Table 2 and Supplementary Fig. S5), with long and shallow eel-like fishes at one extreme and short deep-bodied fishes at the other and it explains just 22.6% of the total shape variation. However, variation within PC2 only occurs in fishes with lower values on PC1, which are relatively narrow-bodied species. Therefore, using the three major dimensions of size

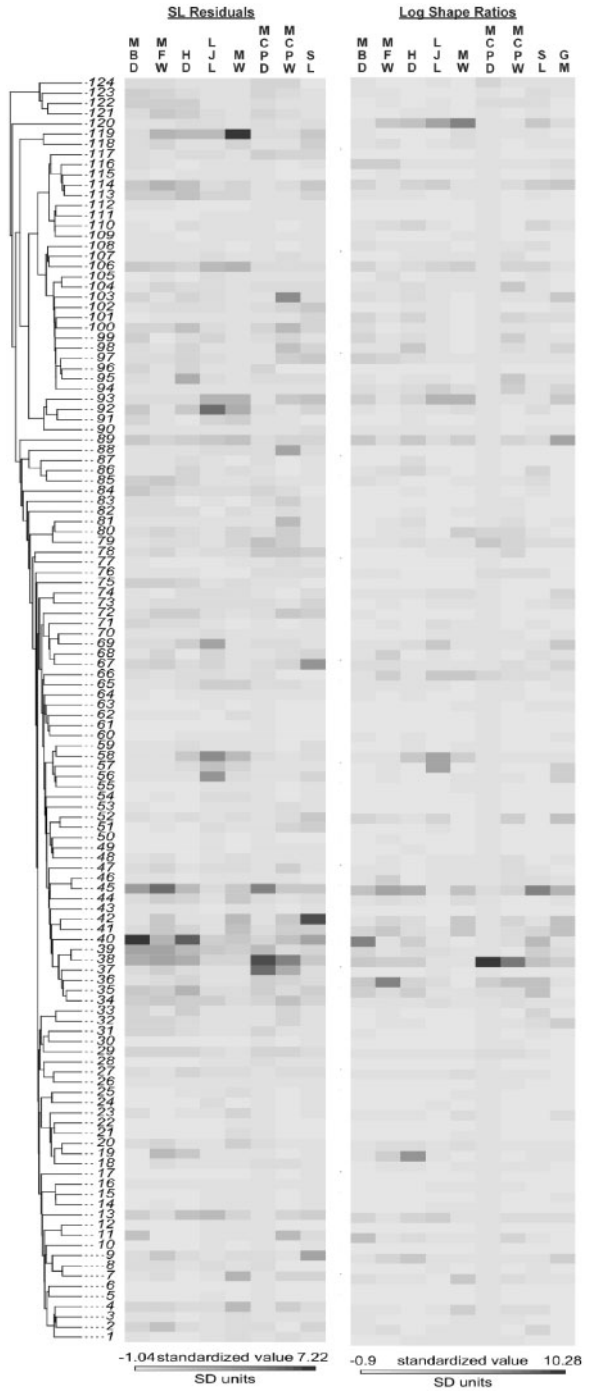

Fig. 2 Standardized per family rates of morphological evolution. Rates of Brownian evolution calculated on log standard length residuals (SLresids) and log-shape ratios (LSRs) within each family that contained at least 10 species in our dataset. Traits are MD, maximum body depth; MFW, maximum fish width; HD, head depth; LJL, lower jaw length; MW, mouth width; MCPD, minimum caudal peduncle depth; MCPW, minimum caudal peduncle width; SL, standard length; GM, geometric mean. Families are: 1, Poeciliidae; 2, Cyprinodontidae; 3, Fundulidae; 4, Goodeidae; 5, Rivulidae; 6, Nothobranchiidae; 7, Exocoetidae; 8, Hemiramphidae; 9, Belonidae; 10, Adrianichthyidae; 11, Melanotaeniidae; 12, Atherinidae; 13, Cichlidae; 14, Blenniidae; 15, Embiotocidae; 16, Pomacentridae; 17, Mugilidae; 18, Soleidae; 19, Paralichthyidae; 20, Pleuronectidae; 21, Sphyraenidae; 22, Centropomidae; 23, Carangidae; 24, Osphronemidae; 25, Channidae; 26, Gobiidae; 27, Eleotridae; 28, Apogonidae; 29, Syngnathidae; 30, Mullidae; 31, Callionymidae; 32, Scombridae; 33, Gempylidae; 34, Cottidae; 35, Agonidae; 36, Liparidae; 37, Hexagrammidae; 38, Zoarcidae; 39, Stichaeidae; 40, Triglidae; 41, Sebastidae; 42, Scorpaenidae; 43, Platycephalidae; 44, Serranidae; 45, Channichthyidae; 46, Nototheniidae; 47, Percidae; 48, Centrarchidae; 49, Percichthyidae; 50, Cirrhitidae; 51, Terapontidae; 52, Kyphosidae; 53, Gerreidae; 54, Sillaginidae; 55, Haemulidae; 56, Lutjanidae; 57, Pomacanthidae; 58, Chaetodontidae; 59, Leiognathidae; 60, Sparidae; 61, Nemipteridae; 62, Lethrinidae; 63, Malacanthidae; 64, Sciaenidae; 65, Acanthuridae; 66, Siganidae; 67, Tetraodontidae; 68, Diodontidae; 69, Monacanthidae; 70, Balistidae; 71, Ostraciidae; 72, Antennariidae; 73, Labridae; 74, Scaridae; 75, Batrachoididae; 76, Ophidiidae; 77, Melamphaidae; 78, Holocentridae; 79, Macrouridae; 80, Gadidae; 81, Moridae; 82, Myctophidae; 83, Synodontidae; 84, Galaxiidae; 85, Stomiidae; 86, Sternoptychidae; 87, Gonostomatidae; 88, Osmeridae; 89, Salmonidae; 90, Cyprinidae; 91, Nemacheilidae; 92, Cobitidae; 93, Catostomidae; 94, Mochokidae; 95, Heptapteridae; 96, Schilbeidae; 97, Pimelodidae; 98, Ariidae; 99, Ictaluridae; 100, Sisoridae; 101, Bagridae; 102, Siluridae; 103, Clariidae; 104, Doradidae; 105, Auchenipteridae; 106, Loricariidae; 107, Callichthyidae; 108, Trichomycteridae; 109, Characidae; 110, Acestrorhynchidae; 111, Bryconidae; 112, Triportheidae; 113, Curimatidae; 114, Prochilodontidae; 115, Anostomidae; 116, Serrasalmidae; 117, Alestidae; 118, Clupeidae; 119, Engraulidae; 120, Mormyridae; 121, Ophichthidae; 122, Congridae; 123, Muraenidae; 124, Anguillidae.

to calculate log shape ratios separates the width axis from the axis that contrasts length and depth. In contrast, using the SL residuals links body depth and width, by forcing all traits to be relative to standard length. There is an important phylogenetic component to elongation, as revealed by the non-phylogenetic PCAs (supplementary Fig. S2 and Supplementary Tables S3 and S4). In non-phylogenetic PCA the SL residuals have very similar loadings on PC1 compared to the phylogenetic PCA but PC1 explains a lot more variation in body shape in the non-phylogenetic PCA (64.8% vs. 45.3%). While in the log shape ratios PC1 and 2 switch, so that the non-phylogenetic PC1 is the elongation axis and it also explains more variation in body shape (39%) than PC1 in the phylogenetic PCA (22.6%).

Our recognition of elongation as an important axis of fish body shape diversification is broadly consistent with previous studies across ecomorphologically disparate clades of teleosteans. A study of morphological variation across almost 3000 reef fish species identified elongation as the dominant axis of shape variation (Claverie and Wainwright 2014). Body elongation was also identified as the secondary axis of diversification within 116

Carangaria following the K–Pg mass extinction (Ribeiro et al. 2018). Similarly, a continuum from relatively long and shallow bodies through to deep and short bodies has also been identified as the primary axis of variation in studies on diverse and morphologically disparate cichlid groups (e.g., 45 species of Tanganyikan cichlids in Clabaut et al. [2007], 27 South American geophagine cichlids in Arbour and Lopez-Fernandez [2013], and 127 Neotropical cichlids in López-Fernández et al. [2013]). This continuum of deep-bodied to elongate was also identified as an important component of the first four principal component axes of morphological variation across 329 morphologically diverse characiform species (Burns and Sidlauskas 2019). These body shape changes are frequently associated with changes in habitat and diet (e.g., Clabaut et al. 2007; Burns and Sidlauskas 2019) often related to the benthic–pelagic axis, with pelagic fishes showing more stream-lined and elongate forms (e.g., Ribeiro et al. 2018). However, across teleosts elongation is likely an adaptation to many different lifestyles not just pelagic habitats (Claverie and Wainwright 2014). Unfortunately, more detailed comparisons are hampered by differences in the way body shape is quantified, with most studies favoring 2D geometric morphometrics on lateral photographs. This means it is impossible for these previous studies to provide support for our log shape ratio results, which identify fish width as the primary axis of body shape variation across teleosts with elongation as the secondary axis of variation constrained within the more narrow-bodied forms.

The more minor axes of shape variation within our dataset emphasize caudal peduncle shape and mouth size. Lower jaw length is an important component of PC2, 3, and 4 when SL residuals are used and PC4 when log shape ratios are used, while mouth width is an important component of PC2 and 4 when SL residuals are used. Mouth size was also identified by Claverie and Wainwright (2014), as a minor contributor to overall morphological variation across reef fishes and snout length was found to be an important component of neotropical cichlid diversification (López-Fernández et al. 2013). We identified fishes with very tapered tail regions (shallow and narrow caudal peduncles), such as rattails (Macrouridae), cutlassfishes (Trichiuridae), and knifefishes (Gymnotiformes), as representing one extreme on PC2 and PC3 when SL residuals are used and PC3 when log shape ratios are used. Elongation of the body with a tapering caudal peduncle is a well-known trait of many deep-sea fishes (Neat and Campbell 2013) as well as freshwater knifefishes (Gymnotiformes). Caudal peduncle shape was not identified as an axis of shape variation in past studies, as tapered tails have only evolved in very specific clades, none of which were included in previous studies. The mixing of mouth size and body dimensions within these axes of variation may indicate that both diet/feeding performance and habitat/locomotor strategies are important drivers of fish body shape evolution, but more detailed analyses are needed to confirm this inference.

Our rate analyses confirm that there is substantial variation in rates of morphological evolution across families (Fig. 2), indeed it would be surprising to find invariant rates at this phylogenetic scale. Interestingly, several of the families identified as having exceptionally high rates of morphological evolution across three or more traits also have unusual ecologies or morphologies. Mormyridae have highly unusual morphologies, as hinted at by their common name. Some species of freshwater elephantfishes have extraordinary heads with large brains and trunk-like jaws and all are weakly electric (Helfman et al. 2008). Channichthyidae (crocodile icefishes) are notothenioid fishes, restricted to freezing or near-freezing Antarctic waters (Kock 2005). Similarly, the highest species diversity of Liparidae (snailfishes) is also found in polar regions, although they have a much wider geographic range occurring in cold deep waters worldwide (Møller et al. 2005). Additionally, several families with high rates of shape evolution: Zoarcidae (eelpouts), Triglidae (gurnards), Liparidae, and Stichaeidae (pricklebacks) are also associated with benthic habitats, which are physically diverse and therefore may provide greater ecological opportunity. Many of these families also contain recent rapid radiations (mormyrids: Carlson et al. 2011; notothenioids: Dornburg et al. 2017). Furthermore, Mormyridae, Zoarcidae, and Liparidae have previously been identified as having exceptional rates of speciation and body size diversification (Rabosky et al. 2013). With the exception of mormyrids these families form a phylogenetic cluster of high rates of shape evolution encompassing the Scorpaeniformes and Notothenioidei (see Fig. 2).

Other families show fast rates of evolution in one or two specific traits. In agreement with past analyses of body size (Rabosky et al. 2013) we identify Salmonidae and Sebastidae as having exceptionally fast rates of size evolution, as measured by the geometric mean of the traits. Chaetodontidae (butterflyfishes) are also identified as having fast rates of lower jaw evolution, which is consistent with the previous finding that jaw elongation is the primary axis of head diversification across the family (Konow et al.

2017). Further research is needed to determine whether rate variation occurs within families and whether elevated rates are linked to morphological or ecological innovations. Moreover, additional investigations are needed to establish whether rate variation influences the results of the other phylogenetic comparative analyses (*sensu* Chira and Thomas 2016), as our current implementations assume a single rate of BM across the tree.

On balance, our preferred method of size correction is the log shape ratios. The composite measure of size enabled us to separate the effects of body depth and width from length, which led to a more complete and nuanced understanding of the teleost morphospace. Moreover, the log shape ratios retain any shape variation due to evolutionary allometry and shape changing predictably with size is an interesting component of shape variation. The allometric relationship was significant due to our large sample size but quite weak for most traits, as the geometric mean never explained more than 4% of the total variation in any trait represented as a log-shape ratio. Such weak evolutionary allometry is consistent with a recent study on the influence of size on the body shape of reef fishes (Friedman et al. 2019) using the geometric morphometric dataset of Claverie and Wainwright (2014). Our identification of positive or negative allometry sometimes depended on whether the phylogeny was taken into account when estimating the linear regression (Supplementary Figs. S6 and S7). It should be noted that we did not attempt to fit non-linear models. Under different circumstances it may be advisable to remove shape variation due evolutionary allometry using the phylogenetic residuals from a regression against size and to do so we would recommend using the geometric mean of the three major size dimensions as the estimate of size.

Large phenotypic datasets promise to revolutionize the fields of genomics and macroevolution (Houle et al. 2010; Chang and Alfaro 2016). Our research demonstrates how these phenomic databases can be built using traditional morphometrics and people power, just as previously observed for crowd-sourcing methods (Chang and Alfaro 2016; Cooney et al. 2017). We also illustrate that careful consideration is needed when analyzing macroevolutionary datasets that span vast taxonomic scales, as choices made when preparing the data for analysis can affect down-stream comparative analyses. In particular, we recommend checking for potential outliers driven by recent sister-taxon nodes and carefully considering the method of size correction. Removing very recent nodes influenced all of our phylogenetic comparative analyses but unsurprisingly the impact was strongest on the rate analyses. After dealing with these issues our analyses reveal that the fastest rates of shape evolution are primarily found within the clade formed by notothenioids and scorpaeniforms in families that thrive in cold waters and/or have benthic habits. The morphospace generated from the log shape ratios revealed that fish width is the primary axis of variation across teleosts, and elongation (depth decreases as length increases) is the secondary axis, occurring only within narrower bodied-fishes. This result highlights the importance of collecting shape on three dimensions, as previous large-scale studies of fish body shape have not included width (Claverie and Wainwright 2014; Chang and Alfaro 2016). In the future, our teleost morphospace will provide context for exploring the nature of adaptive radiations within fishes and allow us to compare fossil and extant diversity.

Acknowledgments

This research would not have been possible without the support of the curators and staff of the Smithsonian National Museum of Natural History Division of Fishes, in particular Kris Murphy, Diane Pitassy, and Sandra Raredon, and the hard work of our large team of researchers, especially those who gave up at least a month of their summer to collect data at the museum*. Our sincere thanks to undergraduate researchers: John Estrada*, Megan Coyne*, Maya Nagaraj*, Allison Proffitt*, Evan Hoeft*, Erin Shen*, Mailee Danao*, Aanchal Bisen, Kasey Brockelsby*, Jo Hsuan Kao*, Laura Vary*, Lauren Maas, Analisa Milkey, Monica Linares*, Victoria Susman*, Justin Waskowiak, Justin Huynh, Kazoua Vang, Lin-Ya Hu, Nikita Hudson, Rebekah Hwang, Hye Yun Lee, Tahmina Tasmin, Timothy Leung, Vivian Nguyen, Xylina Rusit, Sierra Rodriquez*, Brian Landry*, Carley McGlinn*, Nicholas Hix, Brian Kessler, Dominique Gross*, Bailey Benton, Lucas McCutcheon, Hannah Wells, Hannah Whelpley, Mikayla Iwan*, Anna Lee*, Jennifer Nguyen*, and Angelly Tovar*, as well as by the graduate students, lab techs, and other helpers involved in the project: Maxwell Rupp*, Nick Bertrand*, Katerina Zapfe*, and Rachel Friedman*. Also, we wish to acknowledge the incredible work done by the administrative team in the Department of Evolution and Ecology UC Davis that assisted with the logistics of the summer research, in particular: Ruby Wu, Deborah Davidson, and Carla Muñoz. Finally, thanks also to everyone involved in the generation of the large fish phylogeny (Rabosky

et al. 2018) for providing early access to the species lists so we could target our museum data collection.

Funding

This work was supported by the National Science Foundation [grant DEB-1556953 to S.A.P. and P.C.W.], with additional support by the Clemson University Creative Inquiry program for undergraduate research.

Supplementary data

Supplementary data are available at *ICB* online.

References

Albert AYK, Sawaya S, Vines TH, Knecht AK, Miller CT, Summers BR, Balabhadra S, Kingsley DM, Schluter D. 2008. The genetics of adaptive shape shift in stickleback: pleiotropy and effect size. Evolution 62:76–85.

Andersson J. 2003. Effects of diet-induced resource polymorphism on performance in Arctic charr (*Salvelinus alpinus*). Evol Ecol Res 5:213–28.

Andersson J, Johansson F. 2006. Interactions between predator- and diet-induced phenotypic changes in body shape of Crucian carp. 273:431–7.

Arbour JH, Lopez-Fernandez H. 2013. Ecological variation in South American geophagine cichlids arose during an early burst of adaptive morphological and functional evolution. Proc R Soc B Biol Sci 280:20130849.

Arnold SJ. 1983. Morphology, performance and fitness. Am Zool 23:347–61.

Auchincloss LC, Laursen SL, Branchaw JL, Eagan K, Graham M, Hanauer DI, Lawrie G, McLinn CM, Pelaez N, Rowland S, et al. 2014. Assessment of course-based undergraduate research experiences: a meeting report. LSE 13:29–40.

Blake RW. 2004. Fish functional design and swimming performance. J Fish Biol 65:1193–222.

Blake RW, Chatters LM, Domenici P. 1995. Turning radius of yellowfin tuna (*Thunnus albacares*) in unsteady swimming manoeuvres. J Fish Biol 46:536–8.

Burns MD, Sidlauskas B. 2019. Ancient and contingent body shape diversification in a hyperdiverse continental fish radiation. Evolution 73:569–87.

Carlson BA, Hasan SM, Hollmann M, Miller DB, Harmon LJ, Arnegard ME. 2011. Brain evolution triggers increased diversification of electric fishes. Science 332:583–6.

Chang J, Alfaro ME. 2016. Crowdsourced geometric morphometrics enable rapid large-scale collection and analysis of phenotypic data. Methods Ecol Evol 7:472–82.

Chira AM, Cooney CR, Bright JA, Capp EJR, Hughes EC, Moody CJA, Nouri LO, Varley ZK, Thomas GH. 2018. Correlates of rate heterogeneity in avian ecomorphological traits. Ecol Lett 21:1505–14.

Chira AM, Thomas GH. 2016. The impact of rate heterogeneity on inference of phylogenetic models of trait evolution. J Evol Biol 29:2502–18.

Clabaut C, Bunje P, Salzburger W, Meyer A. 2007. Geometric morphometric analyses provide evidence for the adaptive character of the Tanganyikan cichlid fish radiations. Evolution 61:560–78.

Claude J. 2013. Log-shape ratios, Procrustes superimposition, elliptic Fourier analysis: three worked examples in R. Hystrix 24:94–102.

Claverie T, Wainwright PC. 2014. A morphospace for reef fishes: elongation is the dominant axis of body shape evolution. PLoS ONE 9:e112732.

Cooney CR, Bright JA, Capp EJR, Chira AM, Hughes EC, Moody CJA, Nouri LO, Varley ZK, Thomas GH. 2017. Mega-evolutionary dynamics of the adaptive radiation of birds. Nature 542:344–47.

Davis AM, Unmack PJ, Pusey BJ, Pearson RG, Morgan DL. 2014. Evidence for a multi-peak adaptive landscape in the evolution of trophic morphology in terapontid fishes. Biol J Linn Soc 113:623–34.

Domenici P. 2002. Habitat, body design and the swimming performance of fish. In: Bels VL, Gasc JP, Adria Casinos, editors. Vertebrate biomechanics and evolution. Oxford, UK: BIOS Scientific Publishers Ltd. p. 137–56.

Dornburg A, Federman S, Lamb AD, Jones CD, Near TJ. 2017. Cradles and museums of Antarctic teleost biodiversity. Nat Ecol Evol 1:1379.

Felsenstein J. 1985. Phylogenies and the comparative method. Am Nat 125:1–15.

Frédérich B, Sorenson L, Santini F, Slater GJ, Alfaro ME. 2013. Iterative ecological radiation and convergence during the evolutionary history of damselfishes (Pomacentridae). Am Nat 181:94–113.

Fricke R, Eschmeyer W, van der Laan R. 2019. Eschmeyer's catalog of fishes. California Academy of Sciences (https://www.calacademy.org/scientists/projects/eschmeyers-catalog-of-fishes).

Friedman ST, Martinez CM, Price SA, Wainwright PC. 2019. The influence of size on body shape diversification across Indo-Pacific shore fishes. Evolution published online (doi:10.1111/evo.13755).

Froese R, Pauly D. 2019. FishBase (www.fishbase.org).

Gándara P. 1999. Priming the pump: strategies for increasing the achievement of underrepresented minority undergraduates. The College Board's National Task Force on Minority High Achievement 129.

Garland T. 1992. Rate tests for phenotypic evolution using phylogenetically independent contrasts. Am Nat 140:509–19.

Garland T, Harvey PH, Ives AR. 1992. Procedures for the analysis of comparative data using phylogenetically independent contrasts. Syst Biol 41:18–32.

Ghalambor CK, McKay JK, Carroll SP, Reznick DN. 2007. Adaptive versus non-adaptive phenotypic plasticity and the potential for contemporary adaptation in new environments. Funct Ecol 21:394–407.

Gormally C, Brickman P, Hallar B, Armstrong N. 2009. Effects of inquiry-based learning on students' science literacy skills and confidence. Int J Sch Teach Learn 3:Art. 16.

Helfman G, Collette BB, Facey DE, Bowne BW. 2008. The diversity of fishes: biology, evolution, and ecology. Wiley-Blackwell, Chichester UK: John Wiley & Sons.

Hoegg S, Brinkmann H, Taylor JS, Meyer A. 2004. Phylogenetic timing of the fish-specific genome duplication

correlates with the diversification of teleost fish. J Mol Evol 59:190–203.
Houle D, Govindaraju DR, Omholt S. 2010. Phenomics: the next challenge. Nat Rev Genet 11:855–66.
Jungers WL, Falsetti AB, Wall CE. 1995. Shape, relative size, and size-adjustments in morphometrics. Am J Phys Anthropol 38:137–61.
Klingenberg CP. 1996. Multivariate allometry. In: Marcus LF, Corti M, Loy A, Naylor GJP, Slice DE, editors. Advances in morphometrics. NATO ASI Series. Boston (MA): Springer US. p. 23–49.
Klingenberg CP. 2016. Size, shape, and form: concepts of allometry in geometric morphometrics. Dev Genes Evol 226:113–37.
Kock K-H. 2005. Antarctic icefishes (Channichthyidae): a unique family of fishes. A review, Part I. Polar Biol 28:862–95.
Konow N, Price S, Abom R, Bellwood D, Wainwright P. 2017. Decoupled diversification dynamics of feeding morphology following a major functional innovation in marine butterflyfishes. Proc R Soc B Biol Sci 284:20170906.
Kristoffersen JB, Salvanes A. 1998. Effects of formaldehyde and ethanol preservation on body and otoliths of *Maurolicus muelleri* and *Benthosema glaciale*. Sarsia 83:95–102.
Langerhans RB, Chapman LJ. 2007. Complex phenotype–environment associations revealed in an East African cyprinid J Evol Biol 20:1171–81.
Langerhans RB, Gifford ME, Joseph EO. 2007. Ecological speciation in Gambusia fishes. Evolution 61:2056–74.
Langerhans RB, Reznick DN. 2010. Ecology and evolution of swimming performance in fishes: predicting evolution with biomechanics. In: P Domenici, editor. Fish locomotion: an eco-ethological perspective. Boca Raton, FL: CRC Press. P. 200–48.
Lavin PA, Mcphail JD. 1985. The evolution of freshwater diversity in the threespine stickleback (*Gasterosteus aculeatus*): site-specific differentiation of trophic morphology. Can J Zool 63:2632–8.
Lopatto D. 2007. Undergraduate research experiences support science career decisions and active learning. LSE 6:297–306.
Lopatto D. 2009. Science in solution: the impact of undergraduate research on student learning. Tucson (AZ): Research Corporation for Science Advancement.
López-Fernández H, Arbour JH, Winemiller KO, Honeycutt RL. 2013. Testing for ancient adaptive radiations in neotropical cichlid fishes. Evolution 67:1321–37.
Martins EP. 1994. Estimating the rate of phenotypic evolution from comparative data. Am Nat 144:193–209.
Miya M, Pietsch TW, Orr JW, Arnold RJ, Satoh TP, Shedlock AM, Ho H-C, Shimazaki M, Yabe M, Nishida M. 2010. Evolutionary history of anglerfishes (Teleostei: lophiiformes): a mitogenomic perspective. BMC Evol Biol 10:58.
Møller PR, Nielsen JG, Anderson ME. 2005. Systematics of polar fishes. In: John Steffensen and Anthony Farrell, editors. The physiology of polar fishes. Cambridge, Massachusetts: Academic Press. Vol. 22. p. 5–78.
Mosimann JE. 1970. Size allometry: size and shape variables with characterizations of the lognormal and generalized gamma distributions. J Am Stat Assoc 65:930–45.
Moyle PB, Chech JJ. 2004. Fishes: an introduction to ichthyology, fifth edition. Upper Saddle River, NJ: Prentice Hall.
Muschick M. 2012. Convergent evolution within an adaptive radiation of cichlid fishes. Curr Biol 22:2362–8.
Near TJ, Eytan RI, Dornburg A, Kuhn KL, Moore JA, Davis MP, Wainwright PC, Friedman M, Smith WL. 2012. Resolution of ray-finned fish phylogeny and timing of diversification. Proc Natl Acad Sci U S A 109:13698–703.
Neat FC, Campbell N. 2013. Proliferation of elongate fishes in the deep sea. J Fish Biol 83:1576–91.
Orme D, Freckleton R, Thomas GH, Petzoldt T, Fritz S, Isaac N, Pease W. 2018. Caper: Comparative analyses of phylogenetics and evolution in R package version 1.0.1. https://CRAN.R-project.org/package=caper.
Pennell MW, Eastman JM, Slater GJ, Brown JW, Uyeda JC, FitzJohn RG, Alfaro ME, Harmon LJ. 2014. geiger v2.0: an expanded suite of methods for fitting macroevolutionary models to phylogenetic trees. Bioinformatics 30:2216–8.
Polly PD, Lawing AM, Fabre AC, Goswami A, Polly PD, Lawing AM, Fabre AC, Goswami A. 2013. Phylogenetic principal components analysis and geometric morphometrics, the Hystrix. Ital J Mammal 24:33–41.
Rabosky DL, Chang J, Title PO, Cowman PF, Sallan L, Friedman M, Kaschner K, Garilao C, Near TJ, Coll M, et al. 2018. An inverse latitudinal gradient in speciation rate for marine fishes. Nature 559:392–95.
Rabosky DL, Santini F, Eastman J, Smith SA, Sidlauskas B, Chang J, Alfaro ME. 2013. Rates of speciation and morphological evolution are correlated across the largest vertebrate radiation. Nat Commun 4:1958.
Revell LJ. 2009. Size-correction and principal components for interspecific comparative studies. Evolution 63:3258–68.
Revell LJ. 2012. phytools: an R package for phylogenetic comparative biology (and other things). Methods Ecol Evol 3:217–23.
Ribeiro E, Davis AM, Rivero-Vega RA, Ortí G, Betancur-R R. 2018. Post-Cretaceous bursts of evolution along the benthic–pelagic axis in marine fishes. Proc R Soc B Biol Sci 285:20182010.
Robinson BW, Wilson DS, Margosian AS, Lotito PT. 1993. Ecological and morphological differentiation of pumpkinseed sunfish in lakes without bluegill sunfish. Evol Ecol 7:451–64.
Rueden CT, Schindelin J, Hiner MC, DeZonia BE, Walter AE, Arena ET, Eliceiri KW. 2017. ImageJ2: imageJ for the next generation of scientific image data. BMC Bioinformatics 18:529.
Seymour E, Hunter A-B, Laursen SL, DeAntoni T. 2004. Establishing the benefits of research experiences for undergraduates in the sciences: first findings from a three-year study. Sci Educ 88:493–534.
Vandepoele K, De Vos W, Taylor JS, Meyer A, Van de Peer Y. 2004. Major events in the genome evolution of vertebrates: Paranome age and size differ considerably between ray-finned fishes and land vertebrates. Proc Natl Acad Sci U S A 101:1638–43.

Villarejo M, Barlow AEL, Kogan D, Veazey BD, Sweeney JK. 2008. Encouraging minority undergraduates to choose science careers: career paths survey results. LSE 7:394–409.

Webb PW. 1997. Swimming. In: David H. Evans, editor. The physiology of fishes. 2nd ed. Boca Raton, FL: CRC Press. P. 3–24.

Webb PW. 1984. Form and function in fish swimming. Sci Am 251:58–68.

Weihs D. 1993. Stability of aquatic animal locomotion. In: AY Cheer & CP van Dam, editor. Fluid dynamics in biology. Contemporary Mathematics American Mathematical Soc. Providence RI: American Mathematical Society, P. 443–462.

Weihs D. 2002. Stability versus maneuverability in aquatic locomotion. Integr Comp Biol 42:127–34.

West-Eberhard MJ. 2005. Phenotypic accommodation: adaptive innovation due to developmental plasticity. J Exp Zool B Mol Dev Evol 304B:610–8.

Zhao C-M, Kuh GD. 2004. Adding value: learning communities and student engagement. Res High Educ 45:115–38.